

## Simple parameterization of nuclear attenuation data

N. Akopov, L. Grigoryan, and Z. Akopov

*Yerevan Physics Institute, Br. Alikhanian 2, 375036 Yerevan, Armenia*

(Received 13 April 2007; revised manuscript received 26 June 2007; published 6 December 2007)

Based on the semi-inclusive deep inelastic scattering data obtained by the HERMES experiment on deuterium, nitrogen and krypton nuclei, it is shown that a ratio of multiplicities on nucleus and deuterium (per nucleon) for given hadron  $R_M^h$  can be parametrized in a form of a linear polynomial  $a_{11} + \tau a_{12}$ , where  $\tau$  is the formation time, which depends on the energy of the virtual photon  $\nu$  and fraction of that energy  $z$  carried by the final hadron. Three widely known parametrizations for  $\tau$  were used for the performed fit. The fit parameters  $a_{11}$  and  $a_{12}$  do not depend on  $\nu$  and  $z$ .

DOI: [10.1103/PhysRevC.76.065203](https://doi.org/10.1103/PhysRevC.76.065203)

PACS number(s): 13.87.Fh, 13.60.-r, 14.20.-c, 14.40.-n

### I. INTRODUCTION

Semi-inclusive deep inelastic scattering (DIS) of leptons on nuclear targets is a process widely used for studies of hadronization [1–4]. It is most effective to observe at moderate energies of the virtual photon, when the formation time of the hadron is comparable with the nuclear radius.

Hadronization is the process through which partons, created in an elementary interaction, turn into hadrons which are observed experimentally. According to theoretical estimates the hadronization process occurs over length scales that vary from less than a femtometer to several tens of femtometers. Hadronization in a nuclear environment is particularly interesting due to the following reasons. First of all, it allows us to study the parameters governing this process at an early stage; on the other hand, it can provide initial conditions for the investigation of hadronization in hot nuclear matter, which arises in high energy ion-ion collisions.

The most convenient observable measured experimentally for this process is the nuclear attenuation ratio, which is a ratio of multiplicities on nucleus and deuterium (per nucleon) for a given hadron. We shall denote it as  $R_M^h$ . Next step would to find a variable which allows to present this observable in the most simple and convenient form.

For this purpose, the formation time  $\tau$  is proposed as the best variable for  $R_M^h$ , and we shall show that the data can be parametrized in the form of a linear polynomial  $a_{11} + \tau a_{12}$ . Formation time  $\tau$  depends on the energy of the photon  $\nu$  and the fraction of this energy  $z = E_h/\nu$  carried by the final hadron with energy  $E_h$ . Three widely known parametrizations for  $\tau$  were used for the fit procedure. The parameters  $a_{11}$  and  $a_{12}$ , obtained from the fit, do not depend on  $\nu$  and  $z$ . They are functions of the prehadron-nucleon and hadron-nucleon cross sections and the atomic mass number. Experimental data for pions on nitrogen and for identified hadrons on krypton nuclei, obtained by the HERMES experiment [3,4], were used to perform the fit.

This paper is organized as follows. Nuclear attenuation in an absorption model is presented in the next section. In Sec. III we discuss the choice of an appropriate form for the variable  $\tau$ . Section IV presents results of the fit, and conclusions are given in Sec. V.

### II. NUCLEAR ATTENUATION IN ABSORPTION MODEL

The semi-inclusive DIS of lepton on nucleus of atomic mass number  $A$  is

$$l_i + A \rightarrow l_f + h + X, \quad (1)$$

where  $l_i(l_f)$  are the initial (final) leptons, and  $h$  is the hadron observed in the final state. This process is usually investigated in terms of  $R_M^h$ , which is frequently defined as a function of two variables,  $\nu$  and  $z$ :<sup>1</sup>

$$R_M^h(\nu, z) = 2d\sigma_A(\nu, z)/Ad\sigma_D(\nu, z). \quad (2)$$

In experiment it is usually investigated at precise values of one variable and average values of another.

In cases where the  $\nu$ -dependence is studied,

$$R_M^h(\nu, \langle z \rangle) = 2d\sigma_A(\nu, \langle z \rangle)/Ad\sigma_D(\nu, \langle z \rangle), \quad (3)$$

where  $\langle z \rangle$  are the average values of  $z$  for each  $\nu$  bin. And for  $z$ -dependence

$$R_M^h(\langle \nu \rangle, z) = 2d\sigma_A(\langle \nu \rangle, z)/Ad\sigma_D(\langle \nu \rangle, z), \quad (4)$$

where  $\langle \nu \rangle$  are the average values of  $\nu$  for each  $z$  bin.

In this work we adopt a model, according to which the origin of the nuclear attenuation is the absorption of the prehadron (string, dipole) and final hadron in the nuclear medium. In that case  $R_M^h$  has the following form:

$$R_M^h = \int d^2b \int_{-\infty}^{\infty} \rho(b, x) [W(b, x)]^{(A-1)} dx, \quad (5)$$

where  $b$  is the impact parameter and  $x$  the longitudinal coordinate of the DIS point.  $\rho$  is the nuclear density function with a normalization condition:

$$\int \rho(r) d^3r = 1.$$

$W(b, x)$  is the probability that neither the prehadron nor the final hadron  $h$  are absorbed by a nucleon located anywhere in

<sup>1</sup>In fact,  $R_M^h$  also depends on the photon virtuality  $Q^2$  and on the square of the hadron transverse momentum in respect to the virtual photon direction,  $p_t^2$ . However, from the experimental data, it is known that  $R_M^h$  is a much sensitive function of  $\nu$  and  $z$  in comparison with  $Q^2$  and  $p_t^2$ .

the nucleus. For  $W(b, x)$  we use the one scale model proposed in Ref. [5]:

$$W(b, x) = 1 - \sigma_q \int_x^\infty P_q(x' - x) \rho(b, x') dx' - \sigma_h \int_x^\infty P_h(x' - x) \rho(b, x') dx', \quad (6)$$

where  $\sigma_q$  and  $\sigma_h$  are the inelastic cross sections for prehadron-nucleon and hadron-nucleon interactions, respectively. Generally speaking,  $\sigma_q$  is a function of the distance  $x' - x$ ,  $\nu$  and  $z$ .<sup>2</sup> However, a comparison of a simple theoretical models containing  $\sigma_q$  as a parameter [2,6], with the experimental data obtained in different kinematical regions (in particular in different domain of  $\nu$ ), shows that the approximation  $\sigma_q = \text{const}$  leads to a very acceptable agreement with the data. Further, taking into account the qualitative character of this work, we shall use this approximation. In the region of high energies,  $\sigma_h$  are approximately constant for all  $h$ . Numerical values of them for different hadrons will be presented in Sec. IV.  $P_q(x' - x)$  is the probability that at distance  $x' - x$  from the DIS point, the particle is a prehadron and  $P_h(x' - x)$  is the probability that the particle is a hadron. The above-mentioned probabilities are related via a condition

$$P_h(x' - x) = 1 - P_q(x' - x). \quad (7)$$

In an analogy with the survival probability for a particle having lifetime  $\tau$  in a system where it travels a distance  $x' - x$  before decaying,  $P_q(x' - x)$  can be expressed in the form

$$P_q(x' - x) = \exp[-(x' - x)/\tau], \quad (8)$$

where  $\tau$  is the formation time. Substituting expressions for  $P_q(x' - x)$  and  $P_h(x' - x)$  in Eq. (6) one obtains

$$W(b, x) \approx 1 - \sigma_h \int_x^\infty \rho(b, x') dx' + \tau(\sigma_h - \sigma_q) \rho(b, x) \approx w_1(b, x) + \tau(\nu, z) w_2(b, x). \quad (9)$$

In the framework of our assumptions about  $\sigma_q$  and  $\sigma_h$ ,  $W$  depends on  $\nu$  and  $z$  only by means of  $\tau(\nu, z)$ .

The formation time in string models can be divided in two parts (see, for instance, the two scale model presented in Refs. [2,6]). The first part is the constituent formation time  $\tau_c$ , which defines the time elapsed from the moment of the DIS until the production of the first constituent of the final hadron. The second time interval begins with the production of the first constituent until the second one, which coincides with the yo-yo<sup>3</sup> or final hadron production. Comparison with the experimental data shows that in the second interval, the prehadron-nucleon cross section has values close to the hadron-nucleon cross section  $\sigma_h$ . If the difference between these cross sections is neglected, the model is reduced to one scale model with  $\tau = \tau_c$ . In the case of the improved two scale

model of Ref. [6], the prehadron-nucleon cross section reaches hadron-nucleon cross section value during a time interval  $\tau = \tau_c + c \Delta\tau$ , where  $\Delta\tau = z\nu/\kappa$ ,  $\kappa$  is the string tension,  $c$  is the free parameter which defines from fit. In Ref. [6] it is shown that  $c \ll 1$ . The transition to the one scale model takes place at  $c = 0$  and corresponds to  $\tau = \tau_c$ . One should note that any complicated absorption string model, in some approximation, can be reduced to the one scale model presented in Eqs. (6) and (9). Substituting  $W(b, x)$  in  $R_M^h$  we obtain

$$R_M^h \approx \int d^2b \int_{-\infty}^\infty \rho(b, x) (w_1 + \tau w_2)^{(A-1)} dx \approx a_{i1} + \tau a_{i2} + \tau^2 a_{i3} + \dots, \quad (10)$$

where  $i$  is the maximal power of  $\tau$  with which we are limited. Although  $R_M^h$  is a polynomial of  $\tau$  with maximal power  $A - 1$ , it is expected that  $a_{i1} > a_{i2} > a_{i3} > \dots$ . The coefficients  $a_{ij}$  depend on  $A$ ,  $\sigma_q$ ,  $\sigma_h$  and nuclear density. This means, that  $a_{ij}$  are different for different nuclei. For each nucleus  $a_{ij}$  are the same for hadrons with equal values of  $\sigma_h$  (for instance for pions<sup>4</sup> and negatively charged kaons). For fit we use three expressions for  $R_M^h$  as first, second and third order polynomials of  $\tau$ :

$$R_M^h[P_1] = a_{11} + \tau a_{12}, \quad (11)$$

$$R_M^h[P_2] = a_{21} + \tau a_{22} + \tau^2 a_{23}, \quad (12)$$

$$R_M^h[P_3] = a_{31} + \tau a_{32} + \tau^2 a_{33} + \tau^3 a_{34}. \quad (13)$$

In order to get the information on the influence of highest order polynomial forms for  $R_M^h$ ,  $R_M^h[P_4]$  expression also was checked (see Sec. IV).

### III. FORMATION TIME

Equation (10) shows that within our approximation,  $R_M^h$  depends on  $\nu$  and  $z$  only by means of  $\tau(\nu, z)$ . This means, that in our approach  $\tau$  plays a role of a “scaling” variable. In this section we will discuss the physical meaning and possible expressions of the formation time  $\tau$ . There are different definitions for the formation time. We define it as a time scale which is necessary in order that the prehadron-nucleon cross section reaches the value of the hadron-nucleon one. In the literature there are three qualitatively different definitions for  $\tau$ . In the first extreme case it is assumed that  $\tau = 0$  (Glauber approach). In the second extreme case  $\tau \gg r_A$ , where  $r_A$  is the nuclear radius (energy loss model [7]). And at last, in our opinion more realistic definition of the formation time, as a function of  $\nu$  and  $z$  which can change from zero up to values larger than  $r_A$ . Experimental data seem to confirm the fact that at moderate values of  $\nu$  (on the order of 10 GeV) the formation time is comparable with the nuclear size, i.e., the hadronization mostly takes place within the nucleus. This follows from the comparison of the experimental data for  $R_M^h$  obtained in the region of moderate [4] and high [2] energies.

<sup>2</sup> $\sigma_q$  is a function of the formation time  $\tau$  rather than a function of variables  $\nu$  and  $z$  separately.

<sup>3</sup>The yo-yo formation means that a colorless system with valence contents and quantum numbers of the final hadron is formed, but without its “sea” partons.

<sup>4</sup> We do not mention the electric charge of pions, because cross sections of differently charged pions with nucleons, which are of interest to us, are equal.

At moderate energies  $R_M^h$  significantly differs from unity and is a sensitive function of  $\nu$  and  $z$ , at high energies  $R_M^h \approx 1$  and weakly depends on  $\nu$  and  $z$ . For the formation time we shall use expressions which do not contradict the third definition mentioned above. The following expressions are used:

- (i) Formation time for the leading hadron [8], which follows from the energy-momentum conservation law

$$\tau_{\text{lead}} = (1 - z)\nu/\kappa, \quad (14)$$

where  $\kappa$  is the string tension (string constant) with numerical value  $\kappa = 1$  GeV/fm. Indeed, Eq. (14) presents formation time for the hadron produced on the fast end of the string or, which is the same, for the last hadron produced from the string. Hadrons can be produced along the whole length of the string. Among them, the hadrons produced on the fast end have a better chance to avoid interactions in the nucleus.

- (ii) Formation time for the fast hadron, which is composed of characteristic formation time of the hadron  $h$  in its rest frame  $\tau_0$  and Lorentz factor (see, for instance, Ref. [5])

$$\tau_{\text{Lor}} = \tau_0 \frac{E_h}{m_h} = \tau_0 \frac{z\nu}{m_h}, \quad (15)$$

where  $E_h$  and  $m_h$  are the energy and mass of the hadron  $h$ , respectively. Let us briefly discuss the factor  $\tau_0$  following Ref. [9]. Unfortunately, the value of  $\tau_0$  is not well known. The existing estimate [10]  $\tau_0 \approx 1$  fm is nothing but an educated guess. The nonperturbative nature of this number—due to time scales of  $\sim 1$  fm and hadronic size scales of 0.5–1 fm—excludes perturbative evaluation schemes; it is hard to calculate  $\tau_0$  from first principles and formation times cannot be addressed in present lattice QCD simulations. In the opinion of the authors of Ref. [9] formation times can range from 0.3 to 2 fm, depending on the flavor, momentum, and energy of the produced hadrons. However in numerical calculations they, for simplicity, assume that the formation time is a constant in the rest frame of each hadron and that it does not depend on the particle type. They use the value  $\tau_0 = 0.5$  fm. If this assumption is correct, then  $\tau_{\text{Lor}}$  for the kaons is approximately 3.5 times shorter than for the pions at the same values of  $\nu$  and  $z$ . It is well known that  $\sigma_\pi \approx \sigma_{K^-}$ . If kaons have a considerably shorter formation time, they must be absorbed in nuclei considerably more than pions, i.e.,  $R_M^\pi$  must be larger than  $R_M^{K^-}$ . The experiment gives  $R_M^\pi \approx R_M^{K^-}$  [4]. Therefore the definition  $\tau_0 = \text{const}$  (numerical values of parameters do not play a major role in our analysis, see explanation in next section) seems irrelevant in the framework of the absorption model. A more realistic approach would be to consider that  $\tau_0$  is proportional to  $m_h$ . The reason for this is that in the string model the meson (baryon) is represented as a system consisting of a quark-antiquark (diquark) and a gluonic string between them. The energy of the system is transferred by the gluonic string from one parton to another and back. One full cycle lasts a period of  $m_h/\kappa$  which we adopt as  $\tau_0$ . Then  $\tau_{\text{Lor}}$  is a universal quantity

which does not depend on the hadron type. However in Sec. IV we will briefly discuss also the case with  $\tau_0 = \text{const}$ .

- (iii) The formation time following from the Lund string model in Ref. [11] is<sup>5</sup>

$$\tau_{\text{Lund}} = \left[ \frac{\ln(1/z^2) - 1 + z^2}{1 - z^2} \right] \frac{z\nu}{\kappa}. \quad (16)$$

One should note that all three types of formation time have similar behavior with  $\nu$ , but different behavior with  $z$ . At the values of  $z$  typical for the HERMES kinematics ( $z \geq 0.2$ ) the behavior of  $\tau$  defined as in Eqs. (14) and (16) with  $z$  is similar, i.e., they are decreasing with the increase of  $z$ , while  $\tau$  defined as in Eq. (15) is increasing with the increase of  $z$ .

#### IV. RESULTS

Nuclear attenuation data for  $\nu$ - and  $z$ -dependencies of electroproduction of pions on nitrogen and of pions, kaons, protons, and antiprotons on krypton nuclei obtained by the HERMES experiment [3,4] were used to perform the fit. For each nucleus a combined fit was performed for all hadrons having equal cross sections and, consequently, identically absorbed by the nuclear matter (in our approach the prehadron-nucleon cross section does not depend on the type of the final hadron). It is worth mentioning that the inelastic cross sections of corresponding hadrons with nucleons in the moderate energy range ( $E_h \sim 10$  GeV) have the following values:  $\sigma_\pi = \sigma_{K^-} = 20$  mb,  $\sigma_{K^+} = 14$  mb,  $\sigma_p = 32$  mb, and  $\sigma_{\bar{p}} = 42$  mb. As a result, two combined fits were performed for:

- (i) positive and negative pions on nitrogen (26 experimental points from [3]);
- (ii) positive, negative, neutral pions and negative kaons on krypton (63 experimental points from [4]).

And three separate fits for:

- (i) positive kaons on krypton (16 experimental points [4]);
- (ii) protons on krypton (16 experimental points [4]);
- (iii) antiprotons on krypton (14 experimental points [4]).

As it clearly follows from Eqs. (2)–(4), the experimental points corresponding to the  $\nu$ -dependence  $R_M^h(\nu, \langle z \rangle)$ , and  $z$ -dependence  $R_M^h(\langle \nu \rangle, z)$  enter in the fit on equal basis, as values of function  $R_M^h(\nu, z)$  at  $(\nu, z)$  equal  $(\nu, \langle z \rangle)$  and  $(\langle \nu \rangle, z)$ , respectively. For the fit,  $R_M^h$  has been taken in polynomial forms  $R_M^h[P_{1,2,3}]$  [see Eqs. (11)–(13)], and formation times (lengths) as in Eqs. (14)–(16). The results for the reduced  $\chi^2$  denoted as  $\chi^2/\text{d.o.f.}$  are presented in Table I. One can see that for each choice of the formation time and for each nucleus,

<sup>5</sup>Note that this approximation is used only for the sake of convenience. For numerical calculations we use the precise expression for  $\tau_{\text{Lund}}$  following from equation  $\tau_{\text{Lund}} = \tau_y - z\nu/\kappa$  with  $\tau_y$  taken from eq. (4.21) of Ref. [11].

TABLE I. The  $\chi^2/\text{d.o.f.}$  values obtained from polynomial fit.  $P_{1,2,3}$  denote the expressions  $R_M^h[P_{1,2,3}]$  used as fitting functions. The necessary details concerning the data sets used for the fit is given in the text.

Target A	$N_{exp}$	Had.	$\tau_{lead}$			$\tau_{Lor.}$			$\tau_{Lund}$		
			$P_1$	$P_2$	$P_3$	$P_1$	$P_2$	$P_3$	$P_1$	$P_2$	$P_3$
$^{14}\text{N}$	26	$\pi^{+,-}$	1.65	1.72	1.73	1.89	1.95	1.81	1.60	1.67	1.71
$^{84}\text{Kr}$	63	$\pi^{+,-,0}, K^-$	1.67	1.32	1.31	8.71	6.62	5.98	1.41	1.23	1.23
$^{84}\text{Kr}$	16	$K^+$	1.95	1.62	1.70	3.47	3.30	3.14	2.78	2.34	2.52
$^{84}\text{Kr}$	16	proton	1.25	1.24	1.04	8.50	9.08	9.82	2.48	2.28	1.90
$^{84}\text{Kr}$	14	antipr.	1.33	0.89	0.92	2.43	2.37	2.04	1.50	0.94	1.03

the values of  $\chi^2/\text{d.o.f.}$  are close for the polynomial approximations  $R_M^h[P_1]$ ,  $R_M^h[P_2]$ , and  $R_M^h[P_3]$ , which means that the inclusion in consideration of the higher order polynomials of  $\tau$  does not essentially improve the description of the data.

In order to test this, we have also calculated the  $R_M^h[P_4]$  polynomial form and obtained the values of  $\chi^2/\text{d.o.f.}$  close to the ones in case of  $R_M^h[P_3]$ . From Table I one can see that the fit gives unexpectedly good values for  $\chi^2/\text{d.o.f.}$  close to the unity for  $\tau_{lead}$  and  $\tau_{Lund}$ , for  $\tau_{Lor.}$  the agreement is much worse. As it is known from the experiment [3,4],  $R_M^h(\nu, \langle z \rangle)$  increases with increasing  $\nu$ , and  $R_M^h(\langle \nu \rangle, z)$  decreases with increasing  $z$  for all nuclei. Our assumption is that these functions indeed present different representations of the same function, which depends from only one variable  $\tau$ . In turn  $\tau$  is a function of  $\nu$  and  $z$ .

Now let us discuss the figures and, using Eqs. (14)–(16), present  $R_M^h(\nu, \langle z \rangle)$  and  $R_M^h(\langle \nu \rangle, z)$  as functions of  $\tau$ . Experimental points and results of the fit are presented in Fig. 1 for nitrogen and in Figs. 2 and 3 for krypton. Solid points correspond to  $R_M^h(\nu, \langle z \rangle)$  obtained from the experimental data for  $\nu$ -dependence according to Eq. (3), open points to  $R_M^h(\langle \nu \rangle, z)$  from  $z$ -dependence according to Eq. (4). From the figures one can easily note that experimental points for  $R_M^h(\nu, \langle z \rangle)$  and  $R_M^h(\langle \nu \rangle, z)$  as functions of  $\tau$  have the same behavior and approximately coincide when  $\tau_{lead}$  and  $\tau_{Lund}$  serve as the variables. The reason for this is that these variables are approximately proportional to  $\nu$  and  $1 - z$ . In contrary, the variable  $\tau_{Lor.}$  is proportional to  $\nu$  and  $z$ , and as a consequence  $R_M^h(\nu, \langle z \rangle)$  and  $R_M^h(\langle \nu \rangle, z)$  have opposite behavior as functions of  $\tau_{Lor.}$ . This means that without any calculations one can state that  $\tau_{lead}$  and  $\tau_{Lund}$  can serve as “scaling” variables, but  $\tau_{Lor.}$  cannot. For the sake of convenience we have renormalized  $\tau$  to  $x = \tau/\tau(\text{max})$ , where  $\tau(\text{max})$  are the maximum values of  $\tau$  for each set of data and each choice of the  $\tau$  expression.

The range of variation of  $\tau$  and the numerical values for  $\tau(\text{max})$  in all scenarios for the case of pions on krypton are  $4.1 \leq \tau_{Lor.} \leq 10.5$  fm,  $0.67 \leq \tau_{lead} \leq 14.9$  fm,  $0.65 \leq \tau_{Lund} \leq 8.55$  fm. The range for  $\tau_{Lor.}$  is smaller than for the other formation times. The difference will be more significant if we consider the ranges for the points corresponding to  $\nu$ - and  $z$ -dependencies separately. It is also the reason that we see different slopes in different scenarios. Presentation of  $R_M^h$  as a function of  $\tau/\tau(\text{max})$  allows us to place all data in an interval (0, 1). This choice does not influence the results of the fit and the values of  $R_M^h$ . On each of the figures the linear polynomial

is presented  $a_{11} + xa'_{12}$ , with values  $a_{11}$  and  $a'_{12} = a_{12}\tau(\text{max})$  corresponding to the best fit. Solid, dashed and dotted curves represent the  $R_M^h[P_1]$ ,  $R_M^h[P_2]$ , and  $R_M^h[P_3]$  polynomial fit, respectively. One can easily see that the difference between the curves corresponding to  $R_M^h[P_1]$ ,  $R_M^h[P_2]$ , and  $R_M^h[P_3]$  is small for combined fits (see Figs. 1, 2). This difference is more significant for separate fits in  $\tau_{lead}$  and  $\tau_{Lund}$  scenarios, in the region of small  $\tau$ . We do not discuss the possible reasons for this difference because experimental data in this region have large statistical uncertainties. Naturally, it would be very useful to have precise data in this region.

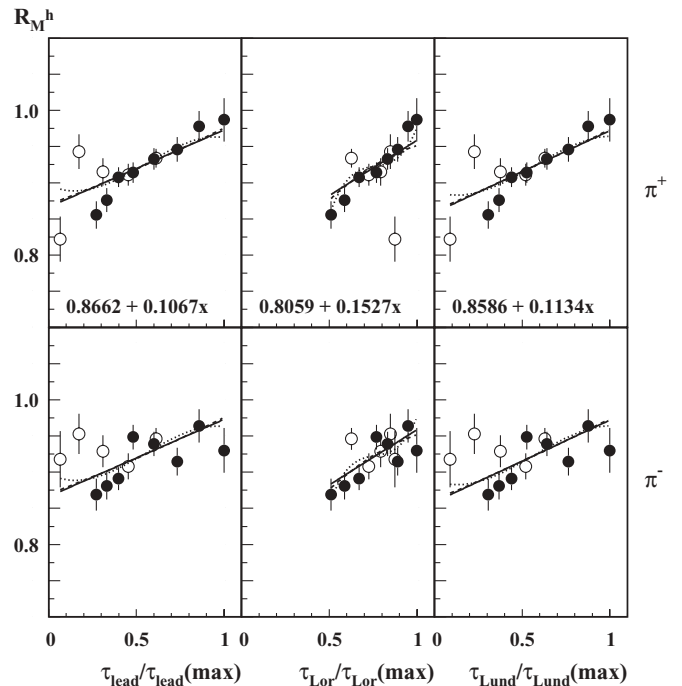


FIG. 1. The values  $R_M^h$  on nitrogen as a function of  $\tau_{lead}$  (left two panels),  $\tau_{Lor.}$  (central two panels),  $\tau_{Lund}$  (right two panels). Normalized values  $\tau/\tau(\text{max})$  for all  $\tau$  are used. On upper panels  $\pi^+$ , on lower  $\pi^-$  mesons are presented, respectively. The open and closed circles are obtained based on the published data [3,4] for  $z$  and  $\nu$  dependencies, respectively. Solid, dashed, and dotted curves are results of linear, quadratic, and cubic polynomial fits. The numerical results for the linear fit are presented on the upper panels.

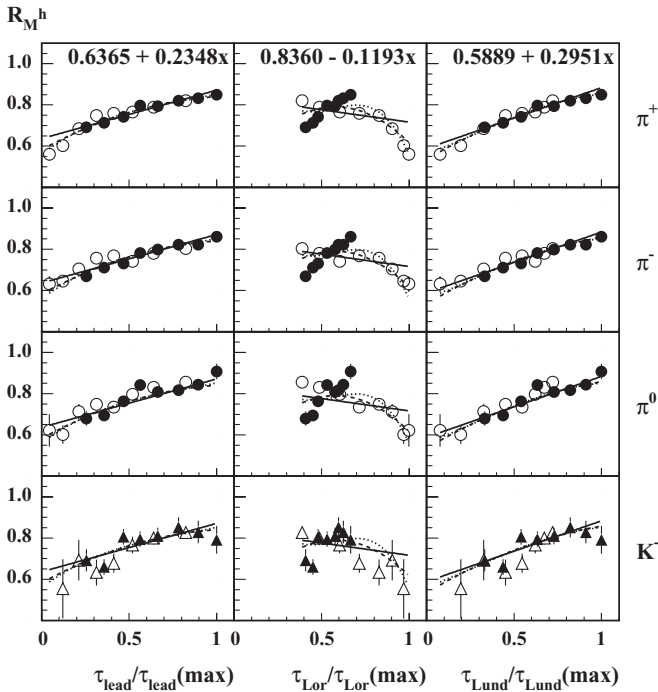


FIG. 2. The values  $R_M^h$  on krypton as a function of  $\tau_{\text{lead}}$  (left four panels),  $\tau_{\text{Lor}}$  (central four panels),  $\tau_{\text{Lund}}$  (right four panels). On panels from upper to lower  $\pi^+$ ,  $\pi^-$ ,  $\pi^0$ , and  $K^-$  mesons are presented, respectively.

The vertical positions of the experimental points are the same in all scenarios. The experimental points can be closer

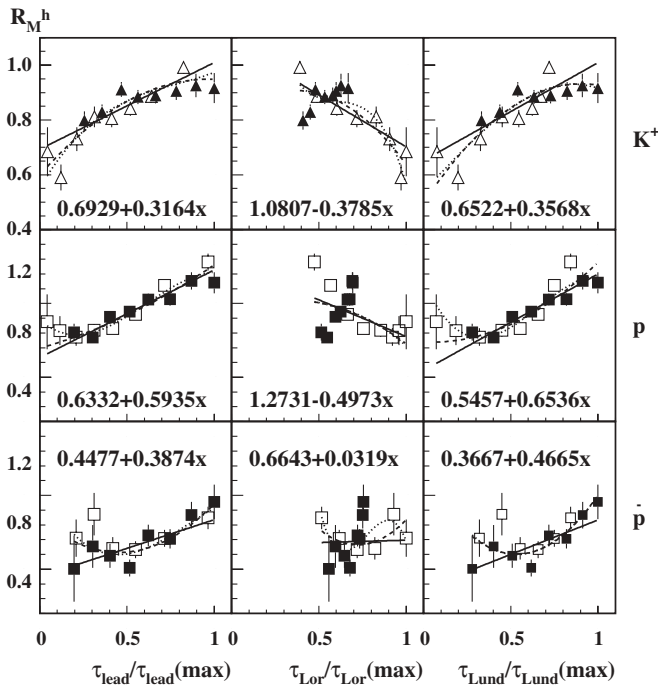


FIG. 3. The values  $R_M^h$  on krypton as a function of  $\tau_{\text{lead}}$  (left three panels),  $\tau_{\text{Lor}}$  (central three panels),  $\tau_{\text{Lund}}$  (right three panels). The results for  $K^+$  mesons are presented in the upper, protons in the middle, and antiprotons in the lower panels.

together (or not) depending on the type of the formation time definition. When looking at the  $\tau$  dependencies, the points corresponding to  $\nu$ -dependence preserve their order in all scenarios. In case of  $z$ -dependence, the order is the same in the scenario with  $\tau_{\text{Lor}}$ , but changes to opposite in other scenarios.

Now let us discuss what would be changed in the results of the present analysis if one uses  $\tau_{\text{Lor}}$  [Eq. (15)] with  $\tau_0 = \text{const}$ . It is quite trivial to see that the results of the combined fit for pions on nitrogen and separate fits for positive kaons, protons and antiprotons on krypton do not change at all. The single difference would be that one cannot now perform a combined fit for the pions and negatively charged kaons. If one excludes kaons from the combined fit on krypton,  $\chi^2/\text{d.o.f.}$  will not change significantly, because kaons do not play an essential role in the fit (statistical uncertainties for kaons are larger than for pions, and the number of experimental points for kaons is essentially smaller than for pions). This means that the results of the fit do not change significantly if Eq. (15) with  $\tau_0 = \text{const}$  is used for  $\tau_{\text{Lor}}$ .

As a last remark, one should note that results of this analysis do not depend from the values of the parameters, in particular from the value of  $\kappa$  (and  $\tau_0$ , if we take  $\tau_0 = \text{const}$ ).

## V. CONCLUSIONS

Nuclear attenuation data for pions on nitrogen and for identified hadrons on krypton nuclei obtained by the HERMES experiment [3,4] were used to perform the fit.

Based on the experimentally measured [3,4] function,  $R_M^h(\nu, \langle z \rangle)$  depends on the variable  $\nu$  only, and  $R_M^h(\langle \nu \rangle, z)$  depends on  $z$  only, and using the published average values of  $\nu$  and  $z$  [3,4] the corresponding values for different representations of the formation length (time)  $\tau$  [see Eqs. (14)–(16)] were used to get the new data sets for  $R_M^h(\tau)$ .

Our main idea is that these functions indeed present different representations of the same function, which depends from only one variable  $\tau$ , which is, in turn, a function of  $\nu$  and  $z$ .

Based on the performed fit of the modified HERMES data (see Table I) we can conclude that the preferable forms used for  $\tau$  are  $\tau_{\text{Lund}}$  [see Eq. (16)] and its approximation for the leading hadrons  $\tau_{\text{lead}}$  [see Eq. (14)]. While the form corresponds to the  $\tau_{\text{Lor}}$  [see Eq. (15)] can be ruled out.

We have demonstrated that  $R_M^h(\tau)$  can, with satisfactory precision, be parametrized in a form of a linear polynomial  $a_{11} + \tau a_{12}$ , where the fitting parameters  $a_{11}$  and  $a_{12}$  do not depend on  $\nu$  and  $z$ .

Sensing possible predictions we can state that the obtained parametrization could be used to describe the data for other experiments like the present Jlab and definitely the upgraded JLab. Also this parametrization could be used to describe the data at the highest energy, although it is known that the attenuation effects are sharply decreased with the energy increasing. In our opinion the HERMES kinematics is the most optimal to apply the proposed approach because of the average formation length in scale of a fermi is compatible with the typical sizes of the nuclei.

- [1] L. S. Osborn *et al.*, Phys. Lett. **B40**, 1624 (1978).
- [2] J. Ashman *et al.*, Z. Phys. C **52**, 1 (1991).
- [3] A. Airapetian *et al.*, Eur. Phys. J. C **20**, 479 (2001).
- [4] A. Airapetian *et al.*, Phys. Lett. **B577**, 37 (2003).
- [5] A. Bialas, Acta Phys. Polon. B **11**, 475 (1980).
- [6] N. Akopov, L. Grigoryan, and Z. Akopov, Eur. Phys. J. C **44**, 219 (2005); hep-ph/0409359 (2004).
- [7] X.-N. Wang and X. Guo, Nucl. Phys. **A696**, 788 (2001); E. Wang and X.-N. Wang, Phys. Rev. Lett. **89**, 162301 (2002).
- [8] B. Kopeliovich, Phys. Lett. **B243**, 141 (1990).
- [9] T. Falter *et al.*, Phys. Lett. **B594**, 61 (2004).
- [10] J. D. Bjorken, Phys. Rev. D **27**, 140 (1983).
- [11] A. Bialas and M. Gyulassy, Nucl. Phys. **B291**, 793 (1987).